

# Inclusive Measurement of the Charmless Semileptonic Branching Ratio of B-hadrons

Pierre Henrard, P. Rosnet

► **To cite this version:**

Pierre Henrard, P. Rosnet. Inclusive Measurement of the Charmless Semileptonic Branching Ratio of B-hadrons. International Conference on High-Energy Physics: ICHEP '96. 28, Jul 1996, Warsaw, Poland. pp.1-11. in2p3-00003986

**HAL Id: in2p3-00003986**

**<http://hal.in2p3.fr/in2p3-00003986>**

Submitted on 17 Feb 2000

**HAL** is a multi-disciplinary open access archive for the deposit and dissemination of scientific research documents, whether they are published or not. The documents may come from teaching and research institutions in France or abroad, or from public or private research centers.

L'archive ouverte pluridisciplinaire **HAL**, est destinée au dépôt et à la diffusion de documents scientifiques de niveau recherche, publiés ou non, émanant des établissements d'enseignement et de recherche français ou étrangers, des laboratoires publics ou privés.

# Inclusive Measurement of the Charmless Semileptonic Branching Ratio of B-hadrons

The ALEPH Collaboration <sup>1</sup>

## Abstract

From the study of the kinematic properties of the final state produced in the semileptonic B decays  $B \rightarrow \ell \nu_\ell X$ , the inclusive charmless semileptonic branching ratio of B-hadrons has been measured. Using the data collected between 1992 and 1995, one gets:  $\text{BR}(B \rightarrow \ell \nu_\ell X_u) = (1.6 \pm 0.4_{\text{stat}} \pm 0.4_{\text{syst}}) \times 10^{-3}$ , where  $X_u$  represents any charmless hadronic state.

## 1 The Method

Charmless semileptonic B meson decays have already been studied in both the exclusive and inclusive channels at the  $\Upsilon(4S)$  (see for instance [1]). The case of exclusive searches is somewhat easier from an experimental point of view because there are more constraints on the final state and because a signal peak can be searched for directly in a mass distribution. The drawback is the large theoretical uncertainties which exist on the knowledge of the hadronic matrix element of the process under consideration. These uncertainties lead to model dependent measurements of the CKM matrix element  $|V_{ub}|$ . Inclusive measurements have been made by looking for an excess of events at the end point of the lepton momentum distribution where the

---

<sup>1</sup>Paper contributed to Warsaw Conference, July 1996



contribution from  $b \rightarrow \ell\nu_\ell c$  vanishes ( $2.3 < p < 2.6$  GeV/c). Starting from this small region of the lepton phase space, an extrapolation to the low momentum region is needed in order to extract the value of  $|V_{ub}/V_{cb}|$ , leading to model dependant measurements.

A possible solution to reduce this model dependence is to use an inclusive measurement with no kinematics cut on the final state  $\ell\nu_\ell X_u$  to ensure a high selection efficiency for  $b \rightarrow u$  transitions. Starting from all these considerations, an inclusive method based on the different kinematics properties of the  $\ell\nu_\ell X_u$  and  $\ell\nu_\ell X_c$  final states has been developed.

## 2 Reconstruction of the boost of the B-hadrons

To reduce the sensitivity of the measurement to the b-quark fragmentation, the analysis is performed in the B-hadron rest frame. This requires to select with a good efficiency all the tracks produced in the final state  $\ell\nu_\ell X$ , and to reject, also with a high efficiency, the tracks coming from fragmentation.

- The lepton ( $e + \mu$ ) identification (with  $p > 3$  GeV/c) and the estimation of the background (from misidentified hadrons, decays, conversions, ...) used in this analysis follow the standard method used in ALEPH for b-physics [2].
- The 3-momentum of the neutrino is determined by using the method given in Ref. [4]. A typical resolution on the neutrino direction of 280 mrad and of 2 GeV on the energy can be obtained.
- The selection of the tracks coming from the hadronic part X is based mainly on the different kinematics properties of tracks from fragmentation and from the B (like the momentum of the track, its rapidity with respect to the lepton axis, etc). It has been done separately for charged tracks and photons by using two neural networks. The two outputs  $NN_\gamma$  and  $NN_c$  for photons and charged tracks are shown in Fig. 1. The better rejection of tracks from fragmentation in the case of charged tracks is due to the additional information given by the impact parameter.

Then, the tracks coming from the hadronic system X are selected by cutting on the  $NN_c$  and  $NN_\gamma$  output with typical efficiencies of 80% and purities of 70% and 60% for  $b \rightarrow c$  and  $b \rightarrow u$  transitions respectively. By using the 3-momenta of the lepton, of the neutrino and of the selected tracks, the boost of a B-hadron decaying into  $\ell\nu_\ell X$  can be computed. The resolutions  $\Delta\theta$  and  $\Delta p_B$  obtained on the direction and on the energy of the B-hadron are :  $\langle \Delta\theta \rangle = 70$  mrad,  $\langle \Delta p_B \rangle = -0.1$  GeV/c and  $\sigma(\Delta p_B) = +4.5$  GeV/c.

## 3 Data analysis

Data events have been selected as follow :

- $q\bar{q}$  events from 1992 to 1995 are selected; this leads to  $3.6 \times 10^6$  hadronic Z decays.

- The cut  $|\cos \theta_{\text{thrust}}| < 0.7$  is applied on the polar angle of the thrust axis to select only events well contained in the detector (this is important to properly calculate the shape variables).

- Events with at least one lepton candidate with  $p > 3 \text{ GeV}/c$  are selected. A pure sample of b-hemispheres is obtained by using a b-lifetime tag in the hemisphere opposite to the lepton [5]. 47675 hemispheres with a lepton (19806 with an electron and 27869 with a muon) satisfy this selection with a b-purity better than 98%.

The simulation of signal  $b \rightarrow u\ell\nu_\ell$  transitions has been done by using the hybrid model of [6] : at low hadronic recoil (below 1.6 GeV), only resonant final states are produced, while for large recoil energy, non-resonant final states are expected to dominate. In this last case, the inclusive ACCMM model is used to predict the invariant mass distribution of the hadronic system X, the  $q^2$  distribution of the W and the lepton momentum spectrum [7].

The separation between the  $B \rightarrow \ell\nu_\ell X_u$  signal decays and the background from  $b \rightarrow c$  transitions has been achieved with the help of a multivariate analysis using a neural network. Since the c quark is heavy compared to the u quark, the  $X_c$  ( $X_c = D, D^*, D\pi, D^*\pi, D^{**}$ ), and  $X_u$  ( $X_u = \pi, \rho, \omega, \eta, f_1, n\pi, \dots$ ) hadronic final states have different shape properties which will be the basis of the definition of the variables used as input of the neural network called in the following  $NN_{bu}$ . In order to get the best possible separation between the  $b \rightarrow u$  and  $b \rightarrow c$  semileptonic transitions, the information from the lepton, the neutrino and from the hadronic system are used. The main physics quantities used to build the input variables are : sphericities, track multiplicity, the energy, invariant masses, the momenta and transverse momenta of tracks, etc. All these quantities are defined from the tracks selected with  $NN_c$  and  $NN_\gamma$  and computed in the reconstructed B-hadron rest frame. One ends up with 20 variables used as input of a 20-15-10-1 multi-layered neural network. The neural network output obtained on simulated events is shown in Fig. 2.

## 4 Results, systematics and checks

The comparison between the data and Monte Carlo is shown Fig. 3 and Fig. 4. In the  $b \rightarrow c$  region (i.e.  $NN_{bu} < 0.5$ ), the agreement obtained between data and Monte Carlo is very good. In the signal region (i.e.  $NN_{bu} > 0.5$ ), there is an excess of  $(267 \pm 90)$  events. This excess of events (the points in Fig. 4) is compatible both in rate and in shape with a  $b \rightarrow u$  probability of the order of 1% (triangles) but is inconsistent with 3% (squares). A fit is made to the region  $NN_{bu} > 0.5$  (this cut leads to the smallest total error and has an efficiency of 60% for  $b \rightarrow u\ell\nu_\ell$ ). The result is  $BR(B \rightarrow \ell\nu_\ell X_u) = (1.6 \pm 0.4_{\text{stat}}) \times 10^{-3}$ , where the statistical error has a  $\pm 0.3 \times 10^{-3}$  contribution from the data and  $\pm 0.2 \times 10^{-3}$  from the limited Monte Carlo statistics.

The sources of the systematic errors and their effects on  $BR(B \rightarrow \ell\nu_\ell X_u)$  are listed in Table 1, leading to the final result :

Source	$\Delta\text{BR}(\text{B} \rightarrow \ell\nu_\ell X_u) \times 10^3$
$\sigma_{\text{stat}}^{\text{lep}^\perp\text{-fit}}$	$\pm 0.25$
$\text{b} \rightarrow \ell$ model	$\pm 0.04$
$\text{B} \rightarrow \text{D}$ model	$\pm 0.02$
$\text{c} \rightarrow \ell$ model	$\pm 0.08$
D topological BR's	$\pm 0.21$
$\text{b} \rightarrow \psi$	$\pm 0.02$
$\text{b} \rightarrow \tau$	$\pm 0.00$
$\text{b} \rightarrow \text{W}$	$\pm 0.01$
$\text{b} \rightarrow \text{u}$ model	$\pm 0.20$
Electron id + background	$\pm 0.02$
Muon id + background	$\pm 0.16$
b and c lifetime eff.	$\pm 0.04$
Total syst. error	$\pm 0.43$

Table 1: Estimated contributions to the systematic uncertainty on  $\text{BR}(\text{B} \rightarrow \ell\nu_\ell X_u)$ . The contribution called  $\sigma_{\text{stat}}^{\text{lep}^\perp\text{-fit}}$  is the error due to the statistical uncertainties on  $\text{BR}(\text{b} \rightarrow \ell)$ ,  $\text{BR}(\text{b} \rightarrow \text{c} \rightarrow \ell)$  and  $\langle X_b \rangle$  from Ref. [3].

$$\text{BR}(\text{B} \rightarrow \ell\nu_\ell X_u) = (1.6 \pm 0.4_{\text{stat}} \pm 0.4_{\text{syst}}) \times 10^{-3}$$

Some checks have been made of the analysis :

- Since this analysis is based on the comparison of the  $\text{NN}_{\text{bu}}$  distribution between data and Monte Carlo, it is important to see how data and Monte Carlo agree in the signal region for background  $\text{b} \rightarrow \text{c}$  hemispheres, in order to be able to attribute the observed excess of events to  $\text{b} \rightarrow \text{u}\ell\nu_\ell$  transitions. This can be done by selecting hemispheres with a lepton and a fully reconstructed D meson into  $\text{K}\pi$ ,  $\text{K}\pi\pi$  and  $\text{K}\pi\pi\pi$ . A very good agreement between the data and the simulation is observed in the signal region giving confidence that the background  $\text{b} \rightarrow \text{c}\ell\nu_\ell$  transitions are well simulated in the region where an excess of events is observed (see Fig. 5).

- The values of  $\text{BR}(\text{B} \rightarrow \ell\nu_\ell X_u)$  obtained for different cuts on  $\text{NN}_{\text{bu}}$  are displayed in Fig. 6. All the points are compatible with the result obtained for the cut  $\text{NN}_{\text{bu}} > 0.5$  within the statistical and systematic uncorrelated error bars. The range of selection efficiencies for  $\text{B} \rightarrow \text{u}\ell\nu_\ell$  covered by the points is from 100% to 24%.

- Even if data and Monte Carlo agree well for the 20 input variables used, possible systematic effects due to the choice of the method used to select the tracks and to the choice of the input variables have been studied. The standard analysis has been changed in the following way : a different algorithm has been used to select the tracks which enter in the definition of the input variables [8]; 15 new variables among the 20 used in the standard analysis have been introduced; the new set of input vari-

ables has been computed in the laboratory frame. This introduces a sensitivity of our result to b-fragmentation which allows for a 2 parameter fit of  $\text{BR}(B \rightarrow \ell\nu_\ell X_u)$  and of  $\langle X_b \rangle$  as a consistency check. As for the standard analysis, the comparison between the data and the simulation without  $b \rightarrow u$  transitions shows an excess of events in the region  $\text{NN}_{bu} > 0.7$ . The one parameter fit (i.e.  $\epsilon_b$  fixed at 0.0035) gives :  $\text{BR}(B \rightarrow \ell\nu_\ell X_u) = (1.5 \pm 0.4_{\text{stat}}) \times 10^{-3}$ , and the two parameter fit leads to :  $\text{BR}(B \rightarrow \ell\nu_\ell X_u) = (1.5 \pm 0.7_{\text{stat}}) \times 10^{-3}$ ;  $\epsilon_b = (3.4 \pm 0.5_{\text{stat}}) \times 10^{-3}$ . The results are in very good agreement with the standard analysis.

## 5 Conclusion

Using an efficient tag based on the kinematic properties of the final states  $B \rightarrow \ell\nu_\ell X_u$  and  $B \rightarrow \ell\nu_\ell X_c$ , the inclusive charmless semileptonic branching ratio of B hadrons has been measured. The analysis of 1992 to 1995 data leads to :

$$\text{BR}(B \rightarrow \ell\nu_\ell X_u) = (1.6 \pm 0.4_{\text{stat}} \pm 0.4_{\text{syst}}) \times 10^{-3}$$

with a little model dependence for the  $B \rightarrow \ell\nu_\ell X_u$  transitions.

## References

- [1] T. Skwanicki, “*Decays of b quarks*”, presented at the XVII International Symposium on Lepton-Photon Interactions, Beijing, China, August 1995.
- [2] D. Buskulic et al., ALEPH Coll., Z. Phys., **C62** (1994) 179.
- [3] P. Perret, talk given at the EPS-HEP-95, Brussel, July 1995.
- [4] H. Duarte, PhD Thesis, Université Paris VI (9 Mai 1994).
- [5] D. Buskulic et al., ALEPH Coll., Phys. Lett. **B313** (1993), 535.
- [6] C. Ramirez et al., Phys. Rev. **D41**, 1496 (1990).
- [7] G. Altarelli et al., Nucl. Phys. **B208** (1982), 365.  
G. Altarelli and S. Petrarca, Phys. Lett. **B261** (1991), 303.  
M. Artuso, Phys. Lett. **B311** (1993), 307.
- [8] This algorithm is described in the paper : R. Akers et al., OPAL Coll., Z. Phys., **C63** (1994) 197-211.

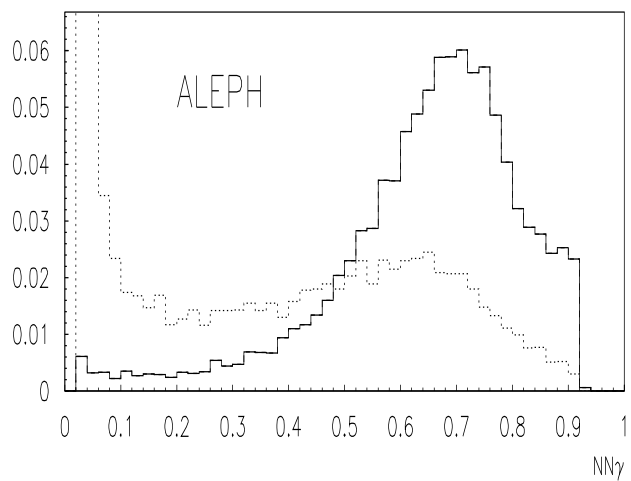
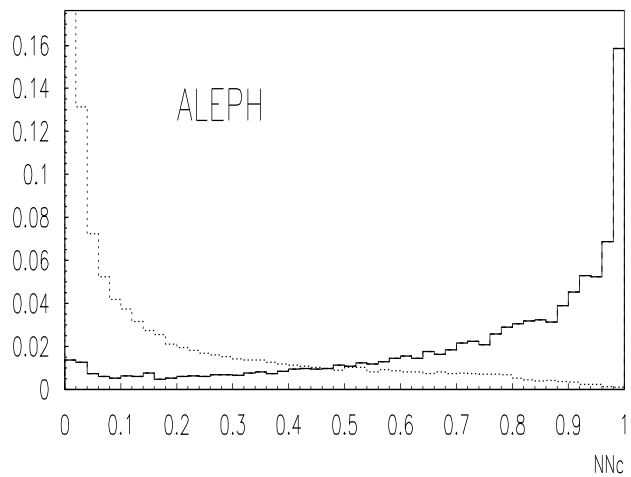


Figure 1: Neural network output for charged tracks (upper plot) and photons (lower plot). The solid histogram is for tracks coming from B decays and the dotted one is for tracks produced in the fragmentation. The two Monte Carlo distributions are normalized to the same area.

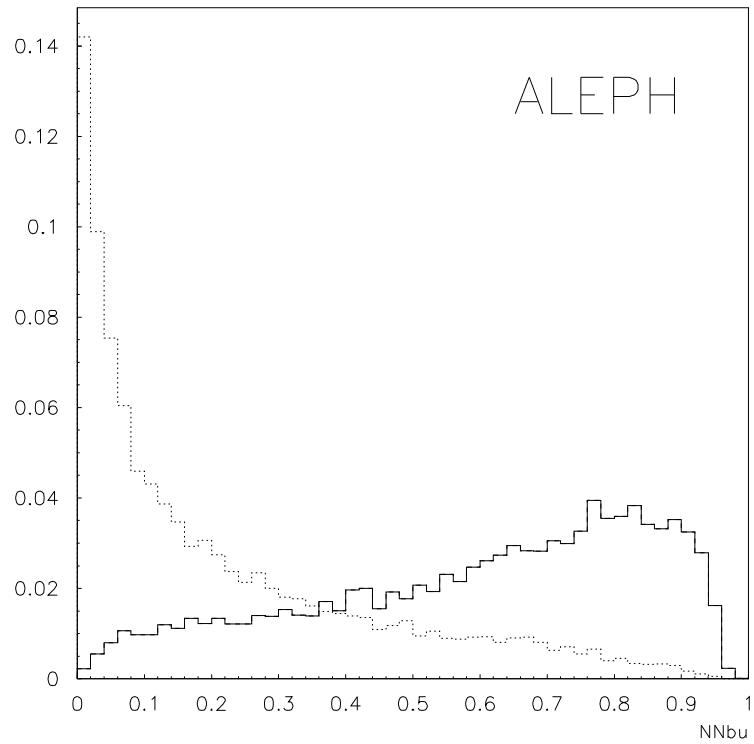


Figure 2: Neural net. output of  $NN_{bu}$  for signal  $b \rightarrow u\ell\nu_\ell$  transitions (solid lines) and background  $b \rightarrow c$  transitions (dotted lines). The two Monte Carlo distributions are normalized to the same area.



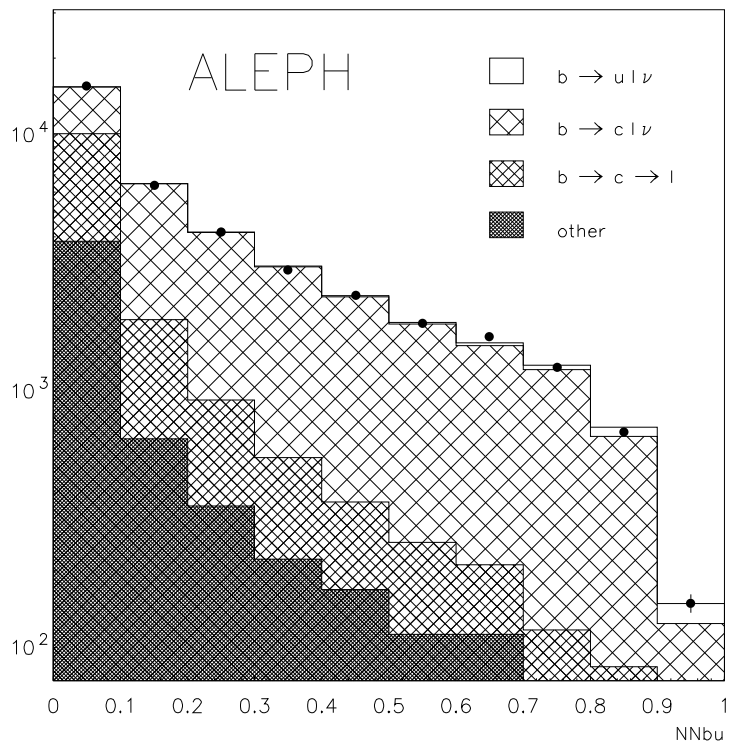


Figure 3: Neural net. output  $NN_{bu}$ ; comparison between data (points) and Monte Carlo (histogram). The two contributions are normalized to the same number of entries.

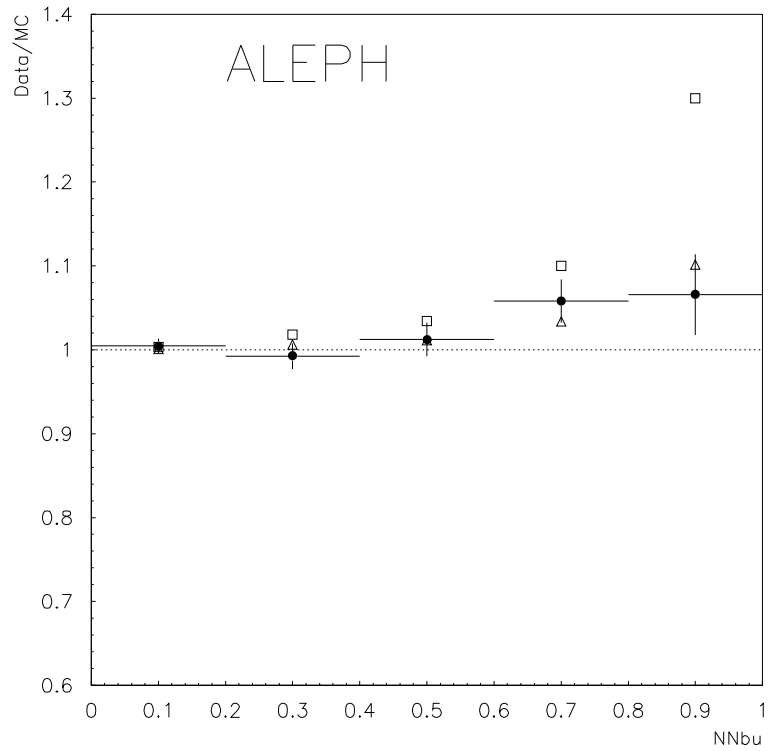


Figure 4: Points : ratio between data and Monte Carlo with no  $b \rightarrow u$  transitions; triangles : ratio between Monte Carlo with the fitted value of  $b \rightarrow u$  and Monte Carlo with no  $b \rightarrow u$  transitions; squares : ratio between Monte Carlo with an arbitrary  $b \rightarrow u$  probability of 3% and Monte Carlo with no  $b \rightarrow u$  transitions.

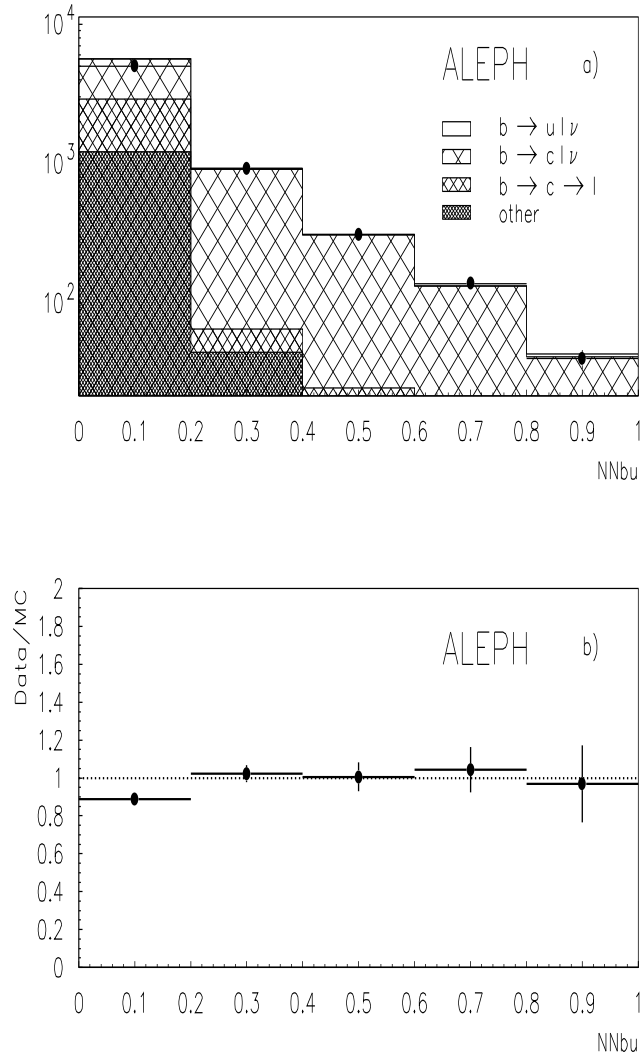


Figure 5: Neural network output  $NN_{bu}$  for hemispheres with a lepton and a reconstructed D meson ( $D^0 \rightarrow K^- \pi^+$  plus  $D^0 \rightarrow K^- \pi^- \pi^+ \pi^+$  plus  $D^+ \rightarrow K^- \pi^+ \pi^+$ ). a) : comparison between data (points) and Monte Carlo (histogram); the first bin is not used to normalize data and simulation since it is dominated by combinatorial background which does not contribute in the signal region; b) : ratio data/Monte Carlo as function of the neural network output  $NN_{bu}$ .

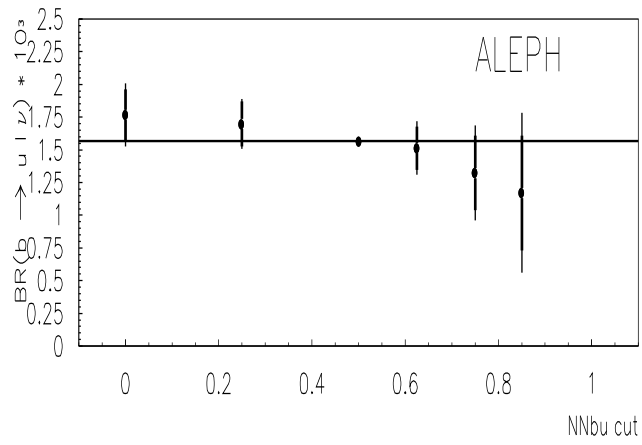


Figure 6: Stability of the measurement of  $\text{BR}(\text{B} \rightarrow \ell \nu_\ell X_u)$  with respect to changing the cut on  $\text{NN}_{\text{bu}}$ . The error bars are the uncorrelated statistical and systematic errors with respect to the cut  $\text{NN}_{\text{bu}} > 0.5$ .